CENP-B preserves genome integrity at replication forks paused by Retrotransposon LTR

Mikel Zaratiegui, Matthew W. Vaughn, Danielle V. Irvine, Derek Goto, Stephen Watt, Jürg Bähler, Benoit Arcangioli, Robert A. Martienssen

Supplementary Information

Supplementary Data

Supplementary Table 1.

sap1-c mutation suppresses slow growth in Δabp1Δcbh1

WT	2.56 (±0.14)
Δcbh1	4.02 (±0.89);
Δabp1	2.74 (±0.21)
Δabp1Δcbh1	11.3 (±2.32)
Δabp1Δcbh1sap1-c	4.77 (±1.72)

Duplication time (hours (±SD)) of haploid strains. 3 independent cultures were grown in rich media at 30ºC and OD readings were taken in 30 minute intervals. The duplication time was calculated for the exponential growth phase (OD between 0.2 and 0.4).

Supplementary Fig. 1

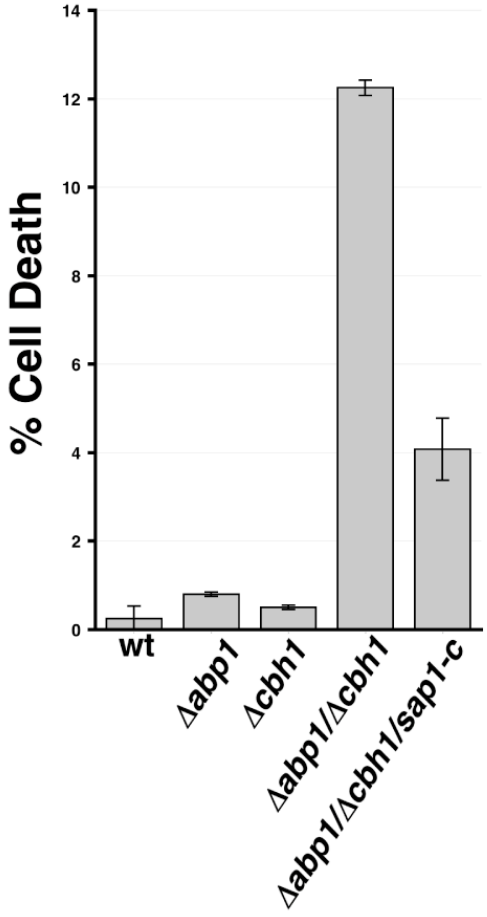

Cell death assays on the indicated mutants. Strains were harvested and analyzed at OD=0.3-0.5. The increased cell death phenotype in the Δ*abp1*Δ*cbh1* mutant is partially suppressed by the *sap1-c* mutation.

Supplemetary Fig. 2

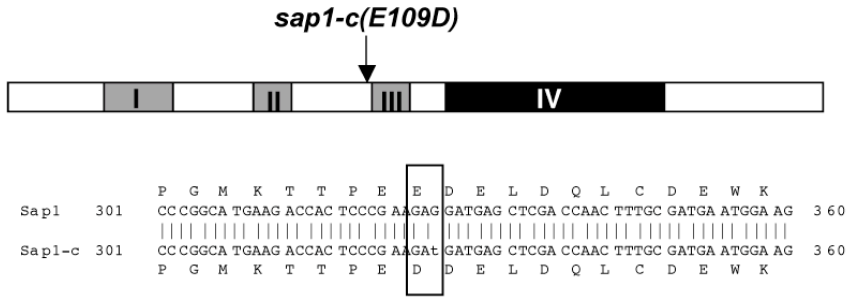

Characterization of the *sap1-c* mutation. a, Location of the *sap1-c* mutation on the coding sequence. Domains I, II and III are DNA binding and Domain IV is the dimerization domain. The *sap1-c* mutation is marked by a rectangle.

Supplementary Fig. 3

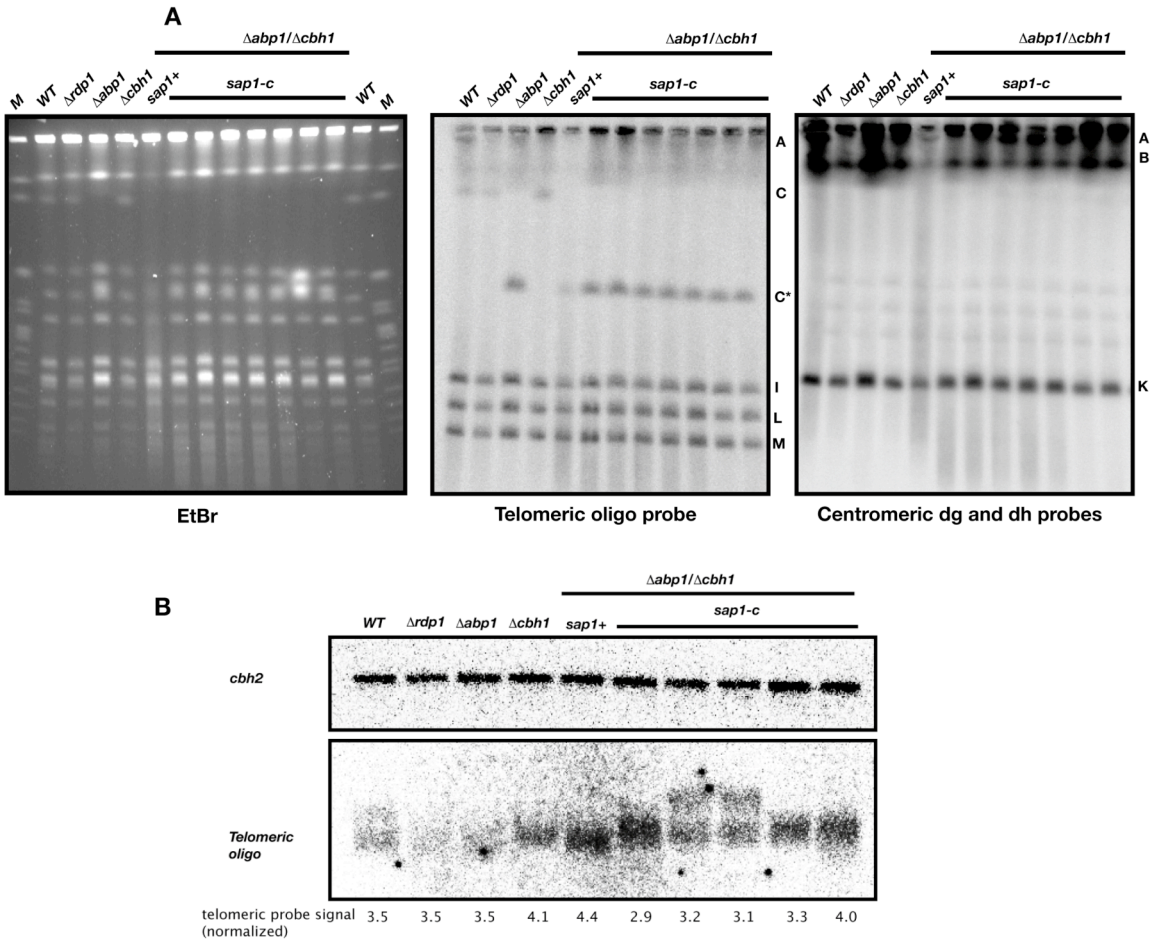

Structural characterization of the genomes on CENP-B and *sap1* mutants. a, Digestion by the rare cutter NotI resolves the fission yeast genome to 17 bands labeled A (complete chromosome III) to Q. Telomere signals are expected from bands A (tel3 L and R), C (tel2 R), I, (tel1 R) L (tel1 L) and M (tel2 L). Band C* results from the digestion of band C into two fragments due to the introduction of a new NotI target by the *abp1* deletion construct. Centromeric signals are expected in bands A (cenIII), B (cenII) and K (cenI). Digestion by NotI releases intact bands from Δ*abp1*Δ*cbh1* agarose plugs indicating recombination or replication intermediates.

B. Quantification of telomeric repeat number and size. Total genomic DNA was subjected to EcoRI digestion, followed by electrophoresis in 1% agarose, southern blotting and hybridisation with a probe against the gene cbh2 or an oligonucleotide complementary to the fission yeast telomeric repeat. Signal from telomeric repeats is in arbitrary units normalized to signal from *cbh2*. In two isolates of Δ*abp1*Δ*cbh1sap1-c* there is a shift in size of telomeric signal that is attributable to a subtelomeric translocation detected by high throughput sequencing.

Supplemental Fig. 4

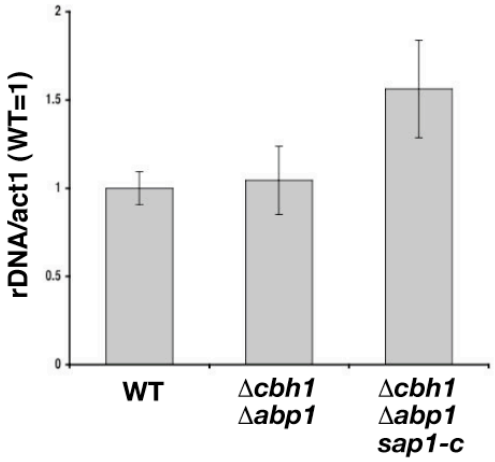

Quantification by Real time qPCR of rDNA copy number. 4 independent colonies of each genotype from WT, Δ*abp1*Δ*cbh1* double mutant and a Δ*abp1*Δ*cbh1sap1-c* triple mutant isolate that showed increased Chromosome 3 size by PFGE (Figure 1) were grown in rich media and the DNA was isolated. Real time qPCR rDNA copy number levels were normalized to *act1* copy number levels, and each data point was normalized to the average of WT copy numbers.

Supplementary Fig. 5

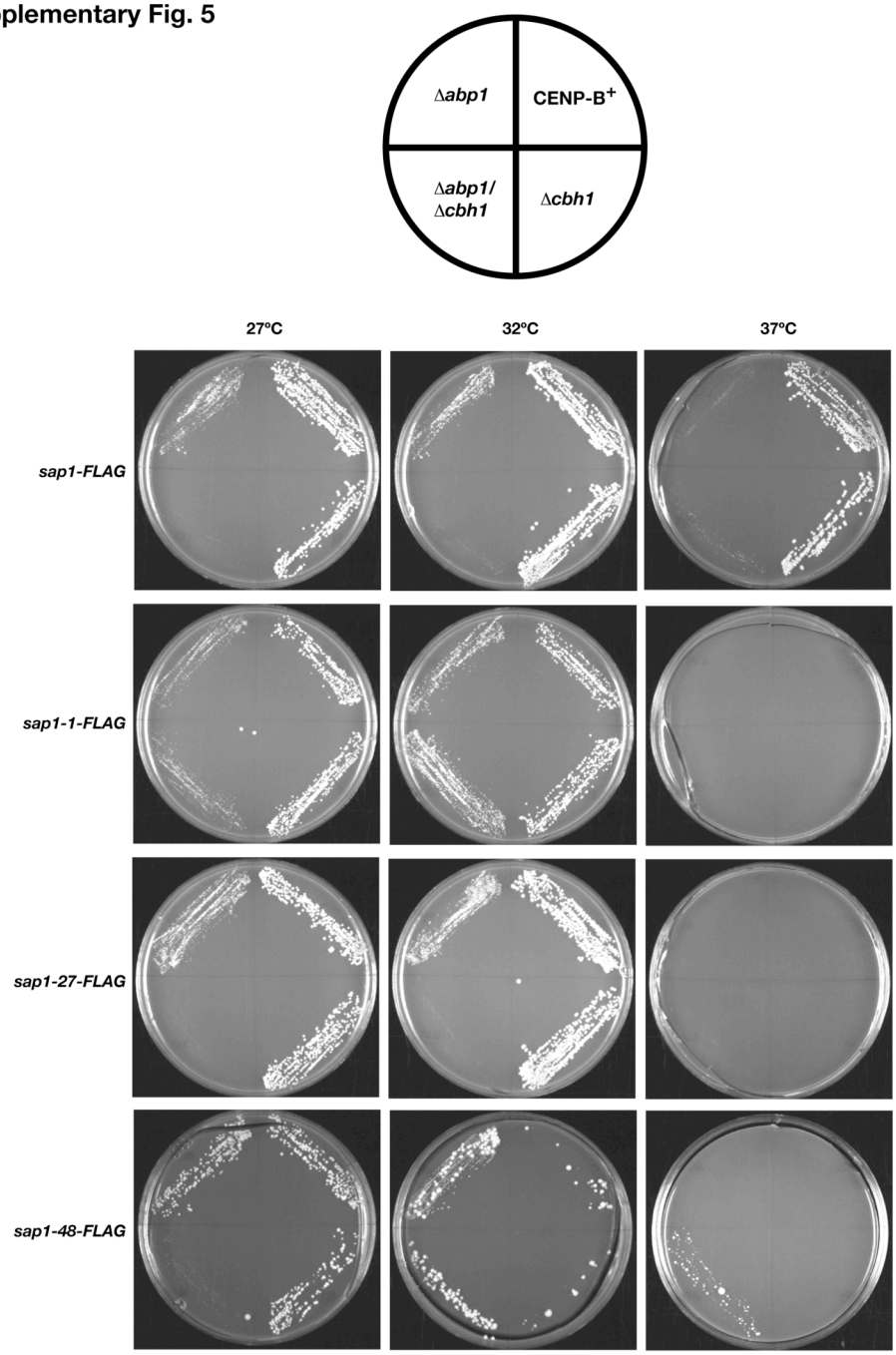

Growth phenotype of CENP-B mutants in combination with sap1 temperature sensitive alleles. Approximately 10^4 cells were streaked onto Rich media and grown for 3 days at the indicated temperatures. While FLAG-tagged *sap1* and the weak allele *sap1-27* do not interact with *abp1* or *cbh1*, *sap1-1* and *sap1-48* suppress the slow growth of Δ*abp1*Δ*cbh1* at the semipermissive temperature. Furthermore, the lethality of *sap1-48* at the restrictive temperature is suppressed by Δ*abp1*Δ*cbh1,* phenocopying *sap1-c* which is only viable in a Δ*abp1*Δ*cbh1* background.

Supplementary Fig. 6

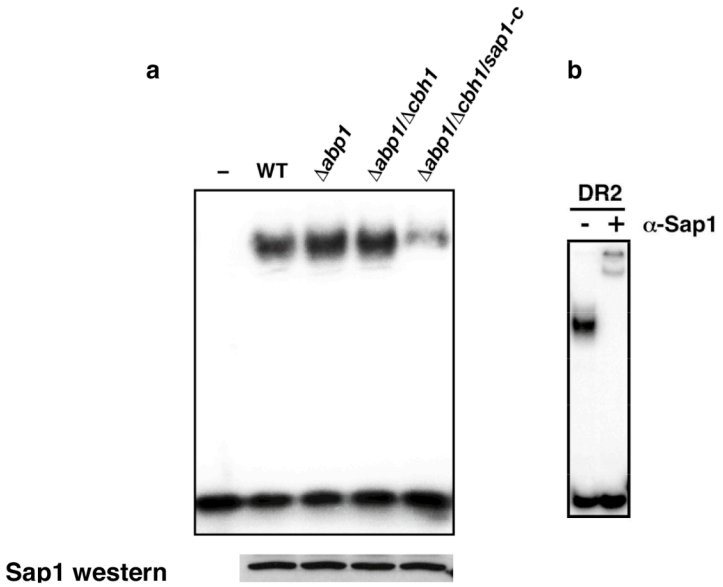

Assay of Sap1 DNA binding activity. a, EMSA (electrophoretic mobility shift assay) of a probe containing the Sap1-binding motif (DR2, see Supplementary Materials and Methods) in extracts from WT, CENP-B mutants (Δ*abp1,* Δ*abp1/*Δ*cbh1*) and CENP-B/sap1 mutants (Δ*abp1/*Δ*cbh1/sap1-c*). b, EMSA of the DR2 probe in the absence (-) or presence (+) of anti-Sap1 serum. The anti-Sap1 serum supershifts the mobility of the bound probe and reduces its abundance, demonstrating that the binding activity in the extract is due to Sap1.

Supplementary Fig. 7

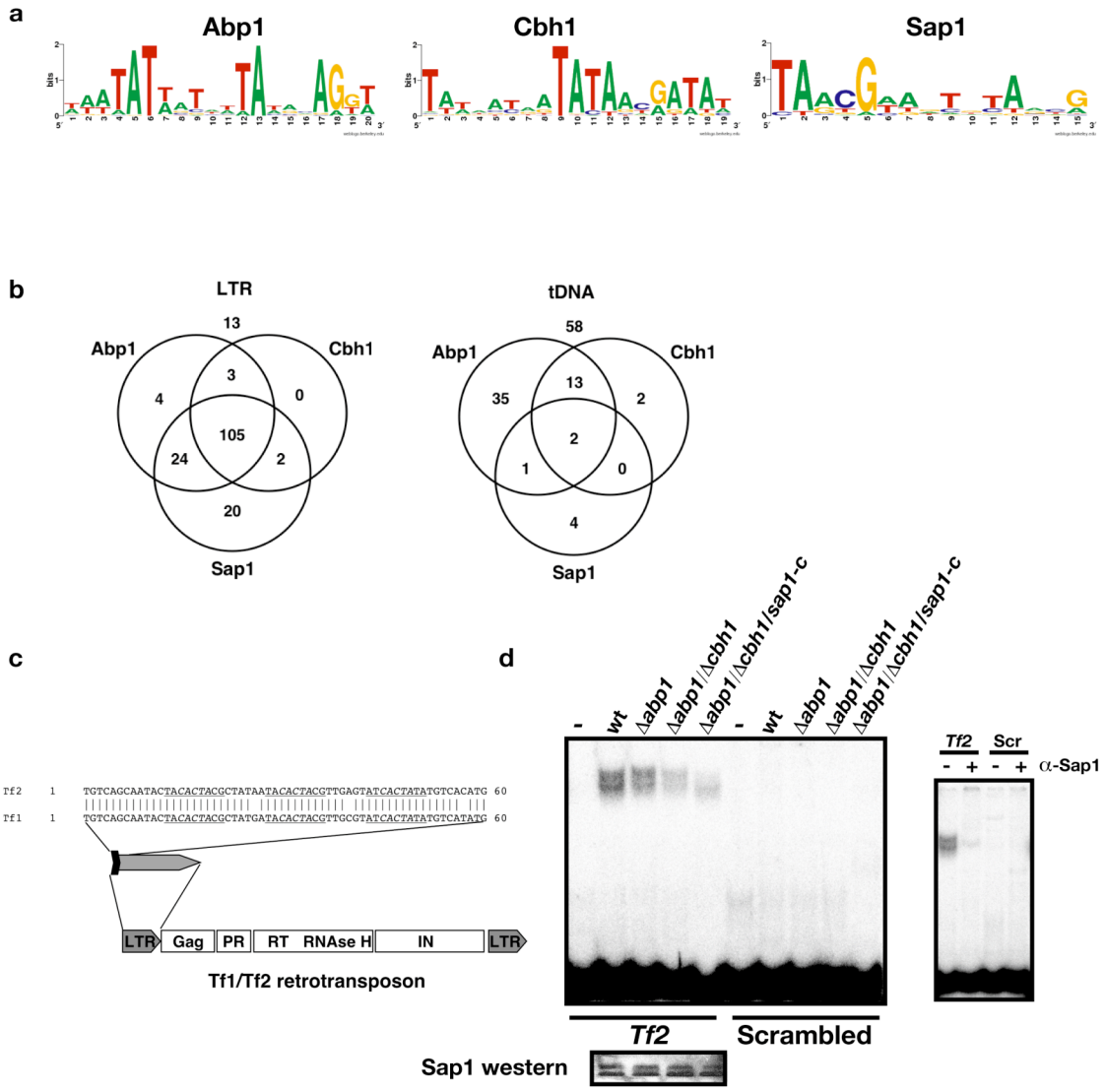

Abp1, Cbh1 and Sap1 binding sites. a, Motifs found by analysis of the sequence of significant peaks in the ChIP-seq. The motifs found in Abp1 and Cbh1 are found in an A/T rich region in the LTR. b, Distribution of Abp1, Cbh1 and Sap1 significant peaks in LTR and tDNA genes. c,Alignment of the 5' end of Tf2 and Tf1 retrotransposon LTR. The putative Sap1 binding sites are underlined. c, EMSA of Tf2 probe and scrambled sequence control probe in extracts from WT, CENP-B mutants (Δ*abp1*, Δ*abp1*Δ*cbh1*) and CENP-B/sap1 mutants (Δ*abp1*Δ*cbh1sap1-c*). Incubation with an anti-Sap1 serum abrogates binding.

Supplementary Fig. 8

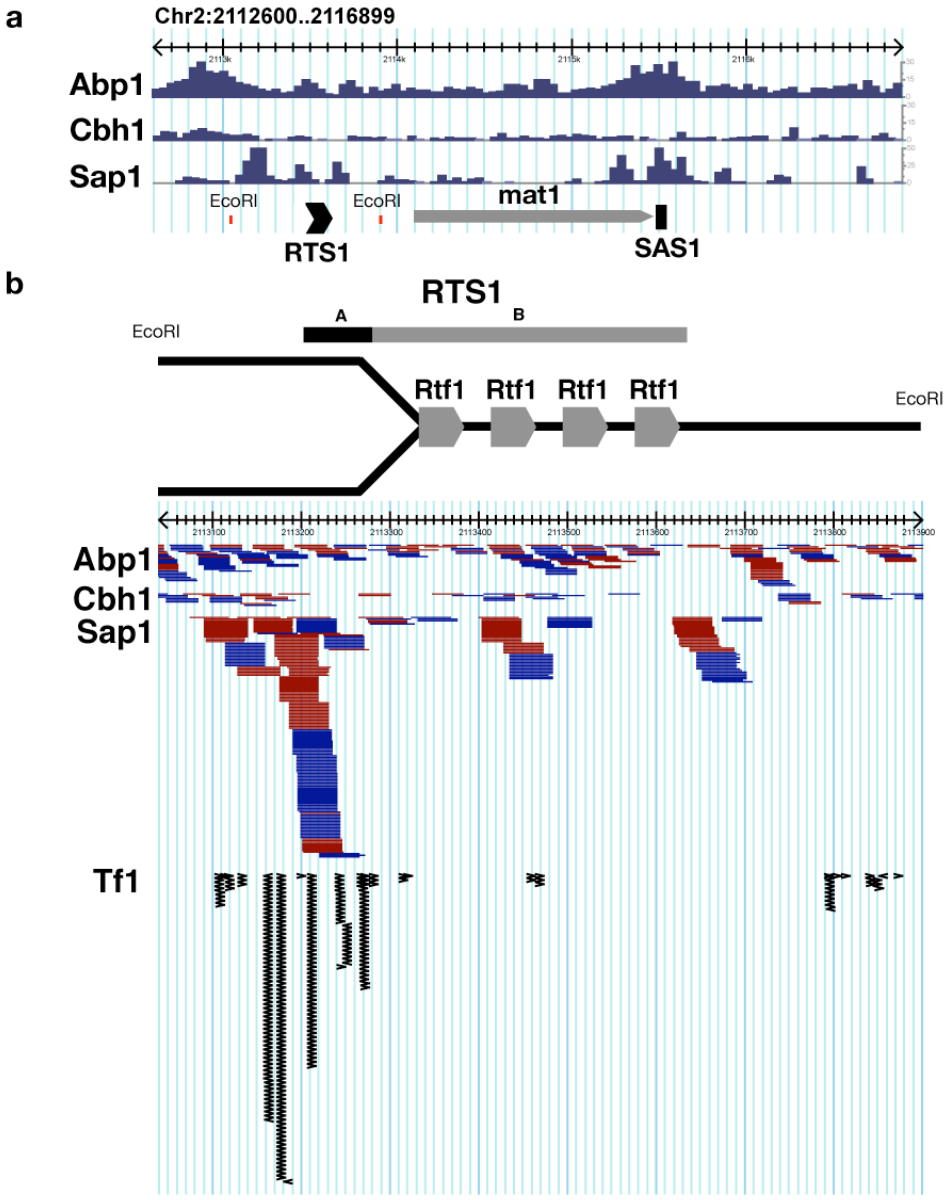

a, ChIP-seq signal at the mat1 locus of the mating type region. RTS1: replication terminator sequence 1. SAS1 Switch Activating Sequence 1. b, Close-up of RTS1, near the mat1 locus at the mating type region. Abp1, Cbh1 and Sap1: ChIP-seq reads with position corrected for peak location (red forward, blue reverse reads). Tf1: position and orientation of Tf1 insertions sequenced in (Guo et al Genome Res 2010). Above, a schematic representation of the region, showing the orientation of the directionality of the replication fork block, as well as the functional components identified in (Codlin et al, EMBO J 2003). Rtf1 binding sites indicated with block arrows. A Sap1 binding site is located in the A region, which enhances the blocking activity of RTS1, and determines the presence of a Tf1 transposition hotspot upstream of the barrier.

Supplementary Fig. 9

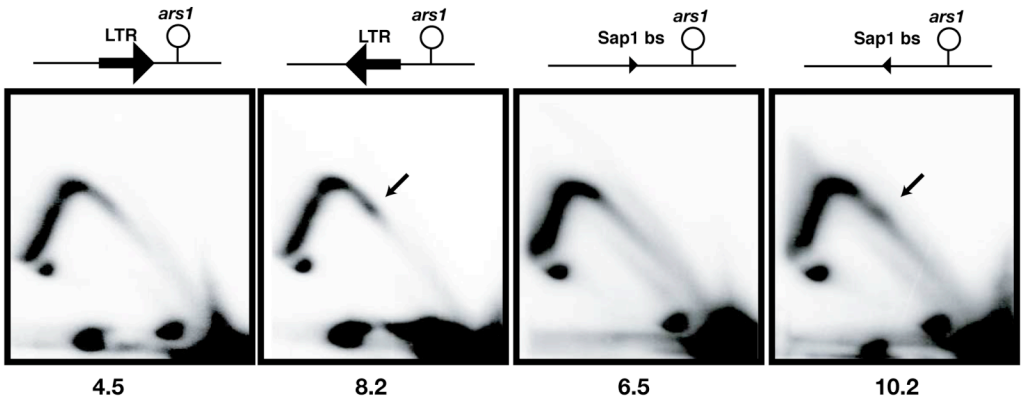

2D gel electrophoresis of plasmid fragments containing the Tf2 LTR or the first 50 base pairs of the Tf2 LTR in both orientations with respect to the ars1 origin, in a WT strain. Accumulation of paused replication intermediates is indicated (arrows). The percentage of hybridization signal within the replication arch over the LTR is indicated below each panel.

The presence of an LTR or the Sap1 binding site in the reverse orientation pauses the replication fork, but not in the forward orientation. This is in agreement with the orientation requirement of the Sap1 binding site present in the Ter1 replication terminator in the rDNA.

Supplementary Fig. 10

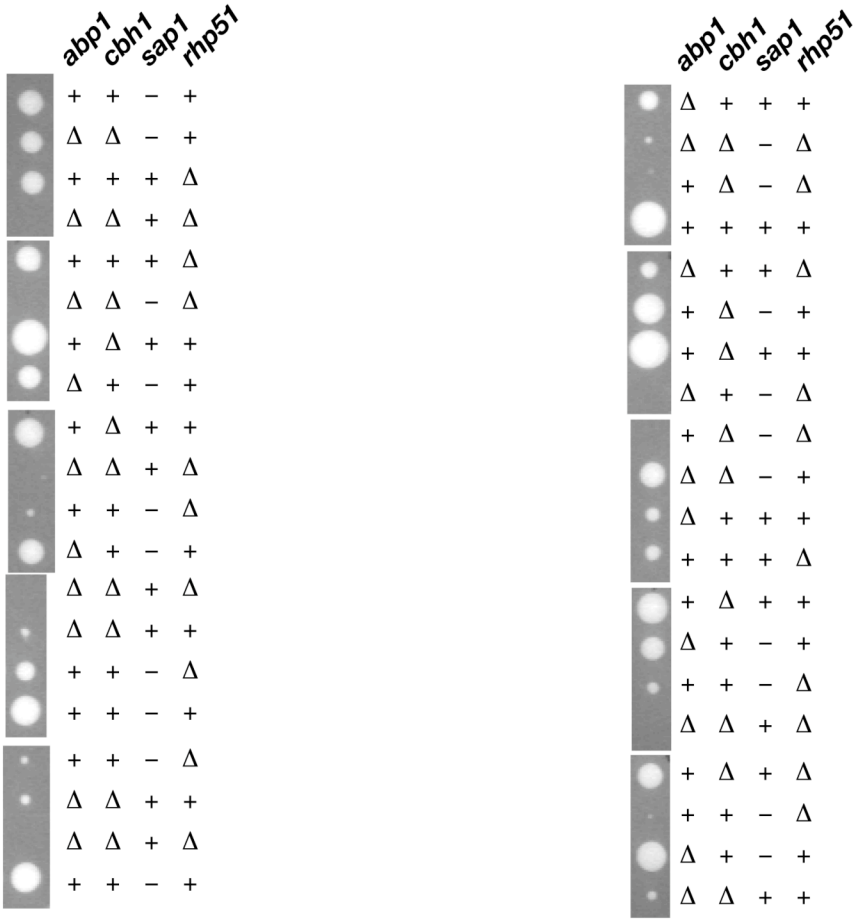

Segregation of a cross between a Δ*abp1*Δ*cbh1sap1-c* triple mutant and a Δ*rhp51* Knockout mutant. Triple Δ*abp1*Δ*cbh1*Δ*rhp51* mutants are inviable, while Δ*abp1*Δ*cbh1*Δ*rhp51sap1-c* quadruple mutants from very slow growing microcolonies. *sap-c*Δ*rhp51* double mutants are also slow growing, suggesting that defective Sap1 function also elicits homologous recombination.

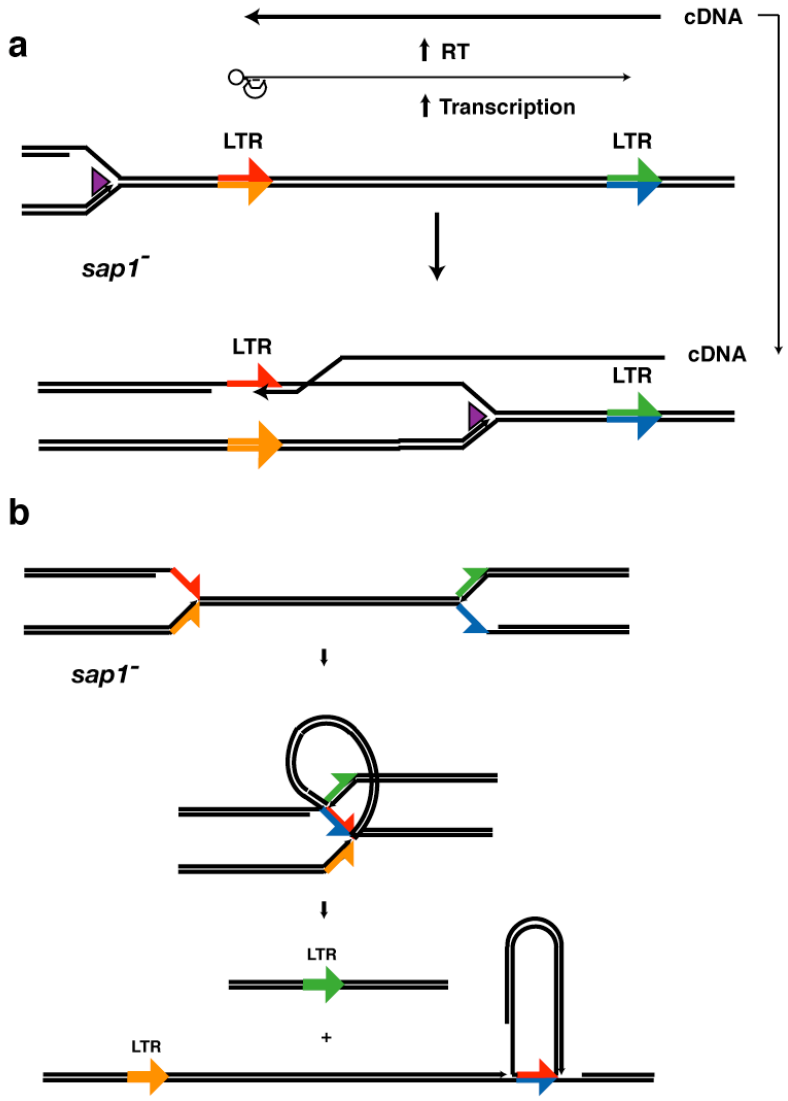

Supplemental Fig. 11

A model for the control of ectopic recombination at LTR by directional replication fork barriers. a. cDNA mediated recombination is promoted by lagging strand replication complementary to the cDNA. b. Inter-LTR recombination could occur by simultaneous replication of both LTR in opposite directions.

Supplementary Methods

Yeast culture

Unless otherwise noted, yeast cultures of haploid strains were grown in YEA media at 30°C to mid-exponential phase, and harvested at an OD600 of 0.5. Genetic manipulation and crosses were performed as previously described [1]. For viability staining, exponentially growing cells were stained with the LIVE/DEAD FungaLight yeast Viability kit (Molecular Probes) according to the manufacturer's instructions. Strains used are detailed in the table below.

Pulsed Field Gel Electrophoresis (PFGE)

DNA plugs for PFGE were obtained using the CHEF yeast DNA plug kit (BioRad) according to the manufacturer's instructions. Proteinase K digestion was allowed to proceed for 48 hours. For molecular karyotyping (whole chromosome electrophoresis), plugs were run in a 0.5x TAE 0.8% Megabase Agarose (BioRad) gel in a CHEF mapper XA apparatus (BioRad). Electrophoresis conditions were: 106° included angle, 30 minutes switch time, 2 V/cm for 72h. After electrophoresis gels were stained with Ethidium bromide, destained and imaged under UV illumination. For blotting, the gel was stained in 1 μg/ml Ethidium Bromide for 30 minutes, exposed to 60 mJoules of UV and denatured in 0.4M NaOH, 1.5M NaCl, then transferred onto Zetaprobe charged Nylon membrane (Biorad) for 48h via capillary transfer with the same buffer. To reveal individual chromosome signals probes for *lys2* (chromosome 1), *act1* (chromosome 2) and *ade6* (chromosome 3) were labeled by random priming (Roche Random Primed

DNA labeling kit), hybridized to the membrane, washed and exposed to phosphorimager screen (Fuji), with stripping by 0.1%SDS 0.1xSSC buffer between individual probes.

Microscopy.

Cells were fixed to glass slides by heat and either observed by Nomarski contrast microscopy or stained for DNA with Vectashield with DAPI (Vector laboratories). Rad22 foci were counted if they were distinctly present as one or several bright spots in the nucleus of the cell. At least 400 nuclei were counted in two independent cultures of each strain. Statistical significance of differences was assessed by multiple Mann-Whitney tests with Bonferroni correction and is depicted as ** $p<0.01$

Chromatin Immunoprecipitation.

ChIP was carried out as previously described [2] with the following modifications. Chromatin was fixed in 3% formaldehyde and sonicated in a Bioruptor (Diagenode). Whole Cell Extract (WCE) DNA was purified in parallel. Immunuprecipitation was performed with anti-Sap1 serum [3] or anti-Calmodulin Binding Protein (for TAP-Cbh1 and TAP-Abp1). PCR was performed in the presence of α-^{32}P-dCTP and run in 5% Acrylamide, 5% glycerol 1xTBE. Quantification of bands was carried out in a phosphorimager and the enrichment calculated as follows: Enrichment= ((test band density in IP)/(reference band in IP))/((test band density in WCE)/(reference band in WCE)). When quantified by qPCR, enrichment was calculated with the same method, using Ct values. The reference amplicon was either *act1* or *ade6*. Experiments were

performed at least in triplicate. Oligonucleotides are detailed in the Oligonucleotides table below.

High throughput sequencing.

For sequencing of the *sap1-c* mutation, two isolates of suppressed mutants were backcrossed three times and two backcrossed strains and a wt sibling were selected for high throughput resequencing. DNA isolation, library construction, sequencing and data analysis were performed as previously described [4]. Candidate mutations were genotyped by DCAPS PCR [5]. For ChIP-seq, immunoprecipitated DNA was polished, ligated and amplified with the Illumina ChIP-seq sample prep kit following to the manufacturer's instructions, and sequenced in an Ilumina G2 analyzer by paired end sequencing. Analysis was carried out by a custom pipeline using MACS 1.3.7.1 for significance enrichment calls [6].

Real time Quantitative-PCR

RTQ-PCR was performed as previously described [7].

ura4 loss assay

12 Independent cultures of the wt and mutant strains were picked from drop-out media without uracil plates to ensure ura4+ starting populations. Cultures were seeded in rich media at the same low density. After growth at 32ºC to saturation they were plated onto 5-FOA selective plates, and grown for 3 days. Dilutions were plated onto rich media to account for possible cell death and plating efficiency. After colonies arose, they were

counted and 96 colonies from each genotype were picked for characterization of the rearrangements by colony PCR with primers ura4#3, Tf2-6F ,Tf2-6R and Tf2_2. 5-FOA resistant colonies that retained the ura4 marker gene were classified as *ura4* mutants. The mutation frequencies were calculated from the mutant counts with the Lea-Coulson Median estimator method[8], and confidence intervals at 95% level were calculated assuming a binomial distribution of mutation frequencies. Statistical significance of differences was assessed by multiple Mann-Whitney tests with Bonferroni correction and is depicted as ** $p<0.01$, n.s. $p>0.05$.

Cloning of constructs for episomal fork pause assay.

We removed the adh1 promoter from the pART2-KanMX6 plasmid (derived from pART1, sequence available upon request) by digestion with BamHI and SphI, and ligation with either the Tf2 LTR, amplified with primer sets LTR_R and LTR_F, or with the first 50 bp of the LTR, obtained by annealing primers S1B_F, S1B_R (_F and _R depict orientation of the insert with respect to the KanMX6 gene). Clones were sequenced to ensure the same sequence on all constructs.

2D gel electrophoresis.

500 ml of the indicated strains grown to OD=0.5 were killed by addition of Sodium Azide to 0.1%, and swirled in centrifuge tubes with 1/3 volumes of frozen 133mM EDTA 33% glycerol until thawed, then harvested by centrifugation, washed with cold sterile water and resuspended in 10 ml Nuclear Isolation Buffer (17% glycerol, 50 mM MOPS pH 7.2, 150 mM potassium acetate, 2 mM $MgCl_2$, 500 μM spermidine and 150 μM

spermine). Cells were spheroplasted by adding 1.5 mg/ml of zymolyase 20T at 37ºC for 30 minutes, lysed by addition of 4 volumes of water then spun at 8000 rpm in a Sorvall SS34 rotor at 4ºC. Pelleted nuclei were resuspended in TEN buffer (50 mM Tris pH8, 50 mM EDTA, 100 mM NaCl) and SDS was added to 0.1%, followed by RNAse A at 0.5 μg/ml and incubation at 37ºC for 30 minutes. Proteinase K was the added to 300 □g/ml and incubated at 37ºC for 60 minutes. SDS was added to a final concentration of 1% continuing incubation at 37ºC for a further 60 minutes. The samples were then cooled in ice for 3 hours, and Potassium Acetate was added to 1.1M continuing incubation in ice for a further hour. Debris was pelleted at 10000rpm in a sorvall SS34 rotor for 10 minutes at 4ºC, and the supernatant was precipitated by addition of 1 volume of isopropanol and immediately centrifuged at 8000 rpm in a sorvall SS34 rotor for 30 minutes at 4ºC. The pellets were resuspended overnight in 5 ml TE, and extracted 5 times in an equal volume of Phenol:Chloroform:Isoamyl Alcohol (25:24:1) and once in Chloroform:Isoamyl Alcohol (24:1) by gentle inversion. The aqueous phase was precipitated by addition of NaCl to 250 mM and 2.5 volumes of Ethanol, followed by incubation at –20ºC for 30 minutes and centrifugation at 8000 rpm in a sorvall SS34 rotor for 30 minutes at 4ºC. Pellets were washed twice in 70% Ethanol and resuspended in 250 μl TE overnight. The purified DNA was the digested with 100 units of PvuII and NcoI (NEB) in the appropriate buffer in a final volume of 400 μl at 37ºC for 6 hours, followed by precipitation with Sodium Acetate at 300mM and 2.5 volumes Ethanol and washing in 70% Ethanol. Pellets were resuspended in 30 μ1x TBE with 1x loading buffer by gentle trituration with wide bore tips.

The sample was loaded in 1.5mm wells. Electrophoresis of the first dimension was carried out in 1X TBE 0.6% agarose (GenePure LE agarose, ISC Bioexpress) at 0.6 V/cm for 40h at room temperature. The gel was stained in 500 μg/L EtBr and the lanes containing the molecular weight marker were illuminated by short wave UV. Sample lanes were cut and excised while protected from UV irradiation, and laid in sample wells cut from 1% agarose 1xTBE gels containing 500 μg/L EtBr. Electrophoresis was carried out at 5 v/cm in 1xTBE 500 μg/L EtBr at 4ºC for 7h. The gel was equilibrated in transfer buffer (1M NaCl, 0.4M NaOH), photographed, and nicked in a UV irradiation box (stratalinker 1800, stratagene) with $4x10^4$ μJ. Transfer was carried out by capillary alkaline transfer overnight onto charged nylon membrane (Hybond XL, GE biosciences). The membrane was crosslinked in a UV irradiation box (stratalinker 1800, stratagene) for $4x10^4$ μJ. Hybridization was performed with Ultrahyb hybridization buffer (Ambion) overnight at 40ºC followed by 2x5 minute washes at the same temperature in 2xSSC 0.1%SDS, and 2x 15 minute washes in 0.1x SSC 0.1% SDS. The probe used was a ClaI digestion fragment of pART2 containing part of the KanMX6 gene labeled with α-p32-dCTP (Perkin-Elmer) by random priming (Roche Random Primed DNA labeling kit). The blots were exposed to phosphorimager screens (Fuji) for 72h and acquired. Quantification or replication arch pauses was carried out with the software ImageGauge (Fuji) by quantifying the signal from the whole replication arch and the signal of the replication arch corresponding to the sizes expected as the fork was traversing the LTR. First, a Region of Interest (ROI) was defined encompassing the signal of the replication arc from the 1n signal to the 2n signal. Then, using the molecular weight markers, limits were placed in the distances that a Y-shaped molecule would migrate in the first

dimension of the 2D electrophoresis (Size of fragment + distance between origin-proximal digestion site to start of LTR, and size of fragment + distance between origin proximal digestion site and end of LTR). The signal within the replication arc that was contained between these two markers was divided by the total replication arc signal and reported as a percentage.

Prediction of binding sites at the LTR

The sequences isolated in the in vitro Sap1 binding selection experiment previously reported[9] were analyzed with the MEME suite[10] and the resulting motif matrix was applied to the consensus Tf1 and Tf2 LTR with the FIMO tool[11]. Similarly, regions significantly enriched as assessed by MACS 1.3.7.1 (see above) were analyzed by MEME to deduce the Sap1, Abp1 and Cbh1 binding sites.

EMSA

To prepare protein extracts 50 ml of the indicated strains were grown at 37ºC in YEA rich media to an OD of 0.5, harvested and washed once in water and once in Extraction Buffer (EB, 50 mM Tris pH8, 300 mM $(NH_4)_2SO_4$, 10mM $MgCl_2$, 5% Glycerol, 14 mM BME, 2 mM PMSF, and Complete Protease Inhibitor tablet (Roche)). The pellet was resuspended in 200 µl EB with 700 µl acid washed 0.5mm glass beads and subjected to bead-beating 3x 30 seconds with 5 minute rests on ice. The extract was filtered from the beads by perforations at the bottom of the tube and low speed centrifugation, and centrifuged at 13k rpm in a tabletop centrifuge for 3 hours. The uppermost third of the supernatant was recovered, quantified for protein content and diluted to equal

concentration (5-8 μg/μl). 2 μl of sample was run on SDS-PAGE and analyzed by western with antibodies against the native Sap1 protein [3]. Mobility shift assays used the probes detailed in the Oligonucleotide tables below. The Forward oligo probes (1.75 pmol) were labeled by Polynucleotide Kinase (NEB) and gamma-32P-ATP (Perkin-Elmer), purified by G25 column (Sigma) and annealed with an equal quantity of Reverse oligo in 10 mM Tris pH8 50 mM NaCl. The binding reaction was carried out between 2 μl of probe and 2 μl of sample in 25 μl reactions (50 mM Tris pH8, 50 mM KCl, 1mM MgCl2, 5% Glycerol, 14 mM BME, 2mM PMSF, Complete Protease Inhibitor tablet, 40 ng/μl salmon sperm DNA) for 5 minutes at room temperature. The reaction was supplemented with anti-Sap1 serum or competing unlabeled probe, in proportions of 1:1, 1:10, 1:100 and 1:1000 labeled probe:unlabeled competitor, where indicated. The samples were then directly loaded into 5% Acrylamide:Bisacrylamide (19:1) gels in 0.5xTBE with 2.5% glycerol, and run at 120V for 2 hours. Gels were then dried and directly imaged with phosphorimager screens (Fuji).

Strains used in this study

Strain name	Genotype	Reference
DG21	*h⁻, otr1R(SphI)::ura4, ura4-DS/E, ade6-216, his7-366, leu1-32*	2
DG124	delta-rdp1::kanMX6, otr1R(SphI)::ura4, leu1-32, ade6-216, his7-366, ura4-DS/E	2
TV340	h-, delta-abp1::leu2+, leu1-32, ura4-DS/E, ade6-210	This study
TV341	delta-cbh1::leu2+, leu1-32, ura4-DS/E, ade6-210	This study
TV418	delta-abp1::leu2+, delta-cbh1::leu2+, ura4-DS/E, leu1-32, ade6-216	This study
FY11012	h-, leu1 ura4, Delta-chk1::ura4	12
FY11110	h-, leu1 ura4, Delta-cds1::ura4	12
ZB392	delta-rad3::kanMX6, otr1R(SphI)::ura4?, ura4-DS/E, ade6-M216, leu1-32, his?	This study
ZB393	delta-tel1::kanMX6, otr1R(SphI)::ura4?, ura4-DS/E, ade6-M210, leu1-32, his?	This study
ZB406	delta-chk1::ura4, Delta-cbh1::LEU2, Delta-abp1::LEU2, his+, ade6+	This study
ZB411	Delta-cbh1::LEU2, Delta-abp1::LEU2, delta-cds1::ura4, his+, ade6+	This study
ZB515	h-, rad22-YFP::KanMX6	13
ZB516	h-, delta-abp1::LEU2, leu1-32, rad22-YFP::KanMX6	This study
ZB517	h-, delta-cbh1::LEU2, rad22-YFP::KanMX6	This study
ZB518	h-, delta-abp1::LEU2, delta-cbh1::LEU2, rad22-YFP::KanMX6	This study
ZB371	h+, delta-abp1::LEU2+, delta-cbh1::LEU2+, ura4-DS/E, leu1-32, ade6-216, sap1-c	This study
4535	h+, sap1-FLAG, leu1-32, ura4-D18	14
4536	h+, sap1-1-FLAG, leu1-32, ura4-D18	14
4537	h+, sap1-27-FLAG, leu1-32, ura4-D18	14
4538	h+, sap1-48-FLAG, leu1-32, ura4-D18	14
ZB542	TAP-abp1:KanMX6, sap1-FLAG, leu1-32, ura4-D18	This study
ZB546	TAP-abp1:KanMX6, sap1-1-FLAG, leu1-32, ura4-D18	This study
ZB549	TAP-abp1:KanMX6, sap1-48-FLAG, leu1-32, ura4-D18	This study
ZB563	Δabp1, sap1-FLAG, leu1-32, ura4-D18	This study
ZB564	Δcbh1, sap1-FLAG, leu1-32, ura4-D18	This study
ZB565	Δabp1, Δcbh1, sap1-FLAG, leu1-32, ura4-D18	This study
ZB566	Δabp1, sap1-1-FLAG, leu1-32, ura4-D18	This study

ZB567	Δcbh1, sap1-1-FLAG, leu1-32, ura4-D18	This study
ZB568	Δabp1, Δcbh1, sap1-1-FLAG, leu1-32, ura4-D18	This study
ZB569	Δabp1, sap1-27-FLAG, leu1-32, ura4-D18	This study
ZB570	Δcbh1, sap1-27-FLAG, leu1-32, ura4-D18	This study
ZB571	Δabp1, Δcbh1, sap1-27-FLAG, leu1-32, ura4-D18	This study
ZB572	Δabp1, sap1-48-FLAG, leu1-32, ura4-D18	This study
ZB573	Δcbh1, sap1-48-FLAG, leu1-32, ura4-D18	This study
ZB574	Δabp1, Δcbh1, sap1-48-FLAG, leu1-32, ura4-D18	This study
PEY905	Tf2-6::ura4, ura4-D18	[15]
ZB557	Δcbh1, Tf2-6::ura4, ura4-D18	This study
ZB558	Δabp1, Tf2-6::ura4, ura4-D18	This study
ZB560	Δcbh1, sap1-c, Tf2-6::ura4, ura4-D18	This study
ZB561	a bp1, sap1-c, Tf2-6::ura4, ura4-D18	This study
ZB528	*h⁻, otr1R(SphI)::ura4, ura4-DS/E, ade6-216, his7-366, leu1-32, pART3-LTRF*	This study
ZB529	*h⁻, otr1R(SphI)::ura4, ura4-DS/E, ade6-216, his7-366, leu1-32, pART3-LTRR*	This study
ZB530	*h⁻, otr1R(SphI)::ura4, ura4-DS/E, ade6-216, his7-366, leu1-32, pART3-S1BF*	This study
ZB531	*h⁻, otr1R(SphI)::ura4, ura4-DS/E, ade6-216, his7-366, leu1-32, pART3-S1BR*	This study
ZB533	h+, delta-abp1::LEU2+, delta-cbh1::LEU2+, ura4-DS/E, leu1-32, ade6-216, sap1-c, pART3-LTRR	This study
ZB536	h-, delta-abp1::leu2+, leu1-32, ura4-DS/E, ade6-210, pART3-LTRR	This study
ZB537	delta-cbh1::leu2+, leu1-32, ura4-DS/E, ade6-210, pART3-LTRR	This study
ZB562	delta-abp1::leu2+, delta-cbh1::leu2+, ura4-DS/E, leu1-32, ade6-216, pART3-LTRR	This study

Oligonucleotides

Riboprobes

lys2	Lys2F	AAAGGTTGCCGATGGTGTAG
	T7Lys2R	TAATACGACTCACTATAGGGAGAGTCAGCATCGCAAAAGACAA
act1	Act1F	AAAGGTTGCCGATGGTGTAG
	T7Act1R	TAATACGACTCACTATAGGGAGAGGAGGAAGATTGAGCAGCAG
ade6	ade6F	TGTAGGGATCCTTGGAGGTG
	T7ade6R	TAATACGACTCACTATAGGGAGAGACCGTCGTAAGCCAATGTT
dh	T7p30F	TAATACGACTCACTATAGGGAGCCTGTTGATTCGGCACCTTTG
	T3p30R	AATTAACCCTCACTAAAGGGAGATGGAGAACGACTGTGAAGAGACC
dg	T7p33F	TAATACGACTCACTATAGGGAGTGCAAGTGGAAAGTGGCTTCA
	T3p33R	AATTAACCCTCACTAAAGGGAGATCGACCACCCTGACTTGTTCTC

PCR (Q-PCR and ChIP-PCR)

act1	act1ChpF	ACTACCGCCGAACGTGAAAT
	act1ChpR	CCTCATGAATACCGGCGTTT
ade6	ade6_9F	TTGACGGAGTTGACTCTCTTCACTC
	ade6_9R	CAGTTATGTCTATGGTCGCCTATGC
LTR	TF2LTRF	TGATAGGTAACATTATAACCCAGT
	TF2LTRR	ACGCAGTTTGGTATCTGATT
tRNA	Cnt3-tRNAF	ACCGTCTGCGAACTGTAAATG
	Cnt3-tRNAR	GGTAGTACACAAGCCTGTCACG
rDNA	rDNAqF	CTGAGAAACGGCTACCACATC
	rDNAqR	GGCCCTGCATTGTTATTTCTT

Transposon eviction assay

TF2-6F	TTCCAGAAATCCAGAAAGAAGC
TF2-6R	CAATTGCAACGTCCAATGAC
Tf2_2	ATTTCAAAAGGGATAACAGTCTTTC

EMSA

Tf2MSf	AGCAATACTACACTACGCTATAATACACTA
Tf2MSr	TAGTGTATTATAGCGTAGTGTAGTATTGCT
scblf	ACAAAATGTCATACGTCTTTAAACCAACAC
scblr	GTGTTGGTTTAAAGACGTATGACATTTTGT
DR2F	GGAATAGCGTGGTGTAGCGAGCCC
DR2R	GGGCTCGCTACACCACGCTATTCC

D-CAPS

sap1F	TCGCAATCAAATCATCTCCA
sap1R	CTTCCATTCATCGCAAAGTTGGTCGAGCTGATC

Episome 2D gel constructs

S1BSF+	TCAGCAATACTACACTACGCTATAATACACTACGTTGAGTATCACTATATG
S1BSFF-	gatcCATATAGTGATACTCAACGTAGTGTATTATAGCGTAGTGTAGTATTGCTGACAtg
S1BSR+	gatcTGTCAGCAATACTACACTACGCTATAATACACTACGTTGAGTATCACTATATGcatg
S1BSR-	CATATAGTGATACTCAACGTAGTGTATTATAGCGTAGTGTAGTATTGCTGACA
LTRFF	ggcatgcTGTCAGCAATACTACACTACGCT
LTRFR	gggatccTGTAAGCTACGCAGTTTGGTATC
LTRRF	gggatccTGTCAGCAATACTACACTACGCT
LTRRR	ggcatgcTGTAAGCTACGCAGTTTGGTATC

References for Supplementary Materials

1. Moreno, S., Klar, A. & Nurse, P. Molecular genetic analysis of fission yeast Schizosaccharomyces pombe. Methods Enzymol 194, 795-823 (1991).
2. Irvine, D. V. et al. Argonaute slicing is required for heterochromatic silencing and spreading. Science 313, 1134-7 (2006).
3. de Lahondes, R., Ribes, V. & Arcangioli, B. Fission yeast Sap1 protein is essential for chromosome stability. Eukaryot Cell 2, 910-21 (2003).
4. Irvine, D. V. et al. Mapping epigenetic mutations in fission yeast using whole-genome next-generation sequencing. Genome Res 19, 1077-83 (2009).
5. Neff, M. M., Turk, E. & Kalishman, M. Web-based primer design for single nucleotide polymorphism analysis. Trends Genet 18, 613-5 (2002).
6. Zhang, Y. et al. Model-based analysis of ChIP-Seq (MACS). Genome Biol 9, R137 (2008).
7. Cam, H. P., Noma, K., Ebina, H., Levin, H. L. & Grewal, S. I. Host genome surveillance for retrotransposons by transposon-derived proteins. Nature 451, 431-6 (2008).
8. Foster, P. L. Methods for Determining Spontaneous Mutation Rates. Methods in Enzymology 409, 195-213 (2006).
9. Ghazvini, M., Ribes, V. & Arcangioli, B. The essential DNA-binding protein sap1 of Schizosaccharomyces pombe contains two independent oligomerization interfaces that dictate the relative orientation of the DNA-binding domain. Mol Cell Biol 15, 4939-46 (1995).
10. Bailey, T. L. & Elkan, C. Fitting a mixture model by expectation maximization to discover motifs in biopolymers. Proc Int Conf Intell Syst Mol Biol 2, 28-36 (1994).
11. Bailey, T. L. et al. MEME SUITE: tools for motif discovery and searching. Nucleic Acids Res 37, W202-8 (2009).
12. National BioResource Project, J.
13. Meister, P. et al. Nuclear factories for signalling and repairing DNA double strand breaks in living fission yeast. Nucleic Acids Res 31, 5064-73 (2003).
14. Noguchi, C. & Noguchi, E. Sap1 promotes the association of the replication fork protection complex with chromatin and is involved in the replication checkpoint in Schizosaccharomyces pombe. Genetics 175, 553-66 (2007).
15. Sehgal, A., Lee, C. Y. & Espenshade, P. J. SREBP controls oxygen-dependent mobilization of retrotransposons in fission yeast. PLoS Genet 3, e131 (2007).